Thermodynamic Analysis of a Waste Heat Integrated Heat Pump–ORC Carnot Battery

Márcio Santos[a], Jorge André[a], Ricardo Mendes[a] and José B. Ribeiro[a]

[a] *ADAI, Department of Mechanical Engineering, Univ Coimbra, Rua Luís Reis Santos, Pólo II, 3030-788 Coimbra, Portugal, marcio.santos@dem.uc.pt, CA, jorge.andre@dem.uc.pt, ricardo.mendes@dem.uc.pt, jose.baranda@dem.uc.pt*

Abstract:

Carnot batteries based on the integration of high-temperature heat pumps (HTHPs) and Organic Rankine Cycles (ORCs) are a promising solution for large-scale energy storage, particularly when coupled with industrial waste heat recovery. This work presents a thermodynamic assessment of Rankine-based HP–ORC Carnot batteries, focusing on the impact of heat pump configuration and working fluid selection. A steady-state model is developed to evaluate key performance indicators, including the coefficient of performance (COP), volumetric heat capacity (VHC), ORC efficiency, and round-trip efficiency, over a range of storage outlet temperatures (90–150 °C) and waste heat source temperatures (40–100 °C). Several heat pump configurations are analysed, from single stage to multi-stage and cascade systems with internal heat recovery. The results show that single-stage configurations are optimal at low to moderate temperature lifts, while multi-stage systems become advantageous at higher lifts. R-601 achieves higher round-trip efficiencies, particularly at elevated temperatures, whereas R-1233zd(E) provides more balanced performance with improved volumetric characteristics. ORC efficiency increases with storage temperature but is limited by turbine off-design behaviour. the results highlight the importance of jointly optimizing system configuration, working fluid, and operating conditions for efficient Carnot battery design.

Keywords:

Carnot battery; High-temperature heat pump; organic Rankine cycle; Waste heat; Thermodynamics.

1. Introduction

The rapid expansion of renewable energy generation, characterized by its inherent variability and intermittency, has intensified the need for efficient and scalable energy storage solutions [1]. In parallel, the decarbonization of industrial and thermal sectors requires technologies capable of bridging the gap between electricity and heat. In this context, large-scale and long-duration energy storage systems are becoming increasingly important to ensure grid stability, enhance energy flexibility, and enable deeper integration of renewable sources across multiple sectors [2]. In industrial environments, the availability of waste heat across a wide range of temperatures further enhances the attractiveness of Carnot batteries. Low- and medium-temperature heat streams, often underutilized, can be upgraded through high-temperature heat pumps (HTHPs) and integrated into thermal storage systems, improving overall system efficiency and reducing energy losses [3]. In this context, heat pump–Organic Rankine Cycle (HP–ORC) configurations have emerged as one of the most promising architectures for waste-heat-assisted Carnot batteries [4].

The performance of these systems is strongly influenced by the thermodynamic efficiency of the charging and discharging subsystems, the operating temperature levels, and the selection of working fluids. In particular, the heat pump plays a dominant role in determining overall system performance, as it directly governs the electrical energy input and the achievable storage temperature. Consequently, the choice of heat pump configuration becomes a key design parameter, especially under large temperature lifts typical of industrial applications.

Considering the Rankine-CB, multiple studies have examined optimal working fluids based on thermodynamic performance and environmental impact. Frate et al. [5] analyzed 17 working fluids, including both artificial and natural options, and found that R1233zd(E) yielded the highest round-trip efficiency, followed by R1234ze(Z) and R717. Dumont and Lemort [6] mapped the performance of a thermally integrated reversible CB with 16 working fluids, determining that R1233zd(E) and R1234yf were most suitable for lower temperature sources, while R245fa provided greater adaptability across a broader temperature range. Zhou et al. [7] investigated working fluid selection for a thermal-integrated Carnot Battery, showing that R1233zd(E)-based zeotropic mixtures improve power-to-power efficiency, reaching 81.26 % in the PR-PTES configuration. The study also emphasizes the importance of optimizing fluid selection for HP and ORC subsystems to minimize exergy losses.

Several studies have compared PTES-based Carnot battery architectures combining basic and recuperated heat pumps with basic and recuperative ORCs. Niu et al. showed that recuperated PTES systems integrated with solar collectors outperform basic configurations, with efficiency increasing as the solar collector area

grows. Frate et al. [8] optimized configurations with and without a regenerator and showed that regeneration increases power-to-power and exergy efficiencies by up to 32% and 19%, respectively. Zhang et al. [9] optimized a Rankine-based Carnot battery operating with R245fa and demonstrated that the inclusion of regeneration reduces the levelized cost of storage by up to 10%.Eppinger et al. [10] investigated recuperated HP–ORC Carnot battery systems using cyclopentane, R365mfc, and R1233zd(E), combined with sensible and latent thermal storage, reporting power-to-power efficiencies between 33% and 82% for a heat source temperature of 80 °C.

Based on the literature, numerous studies have investigated the performance of Carnot batteries with respect to working fluid selection and system configuration. These studies highlight that both fluid selection and system configuration significantly affect system performance, particularly under varying operating conditions. However, despite the growing body of literature, a systematic comparison of advanced high-temperature heat pump configurations within HP–ORC Carnot batteries remain limited. In particular, the combined impact of heat pump architecture, low-GWP working fluid selection, and realistic component behaviour under off-design conditions has not been comprehensively assessed at system level.

In this context, the present work aims to evaluate the thermodynamic performance of waste-heat-assisted Carnot batteries by systematically analysing different high-temperature heat pump configurations and working fluids. A steady-state modelling framework is developed to assess key performance indicators, including the coefficient of performance, volumetric heat capacity, and round-trip efficiency, over a wide range of operating conditions. The results provide design guidelines for the selection of heat pump architectures and working fluids in industrial Carnot battery applications.

2. System Description and Modelling Approach

2.1. System overview

The system investigated in this work is a Rankine-based Carnot battery integrating a high-temperature heat pump (HTHP) for the charging process and a recuperative Organic Rankine Cycle (ORC) for discharging, as illustrated in Figure 1. During charging, surplus electrical energy drives the heat pump to upgrade low-temperature waste heat to a higher temperature level, which is stored in a two-tank sensible thermal energy storage system. During discharge, the stored heat is used to generate electricity through the ORC.

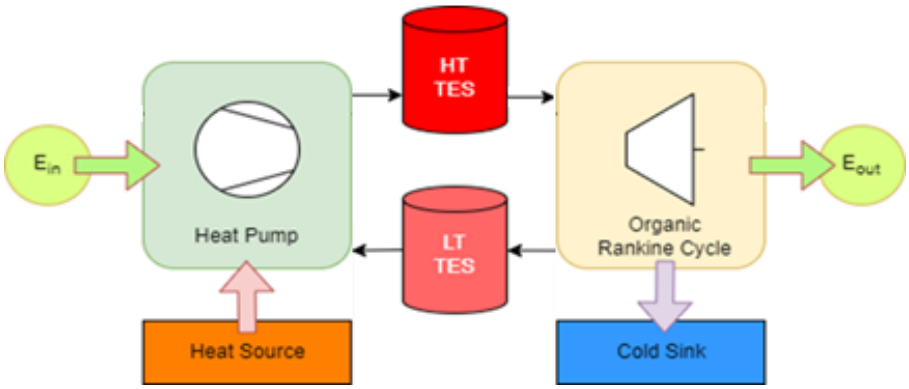

Figure. 1. *Operating principle of a he HP–ORC-based Carnot battery.*

The analysis focuses on industrial waste heat sources in the range of 40–100 °C, representative of low-grade heat streams commonly available in industrial processes. The upgraded heat is delivered at temperatures between 90 and 150 °C, enabling its use in both thermal storage and subsequent power generation.

Several heat pump configurations are considered, including single-stage (SS), single-stage with internal heat exchanger (SS-IHX), two-stage (TS), two-stage with internal heat exchanger (TS-IHX), two-stage with flash tank (TS-IHX-FT), and cascade systems, as shown in Figure 2. These configurations are selected to evaluate the impact of compression staging and internal heat recovery on system performance under varying temperature lifts.

The operation of the single-stage heat pump (Fig. 2a) is illustrated as a reference configuration. The working fluid absorbs heat from the waste heat source in the evaporator and is then compressed, increasing its pressure and temperature. The high-pressure fluid releases heat in the condenser to the thermal storage, upgrading the temperature level. Finally, it expands through a throttling valve, reducing its pressure and temperature before returning to the evaporator, completing the cycle. A series of modifications were implemented to improve the performance of the heat pump. These include the incorporation of a regenerator (Fig. 3b), a two-stage heat pump (Fig. 3c), a two-stage heat pump with regenerator (Fig. 3d), a two-stage heat pump with flash tank and regenerator (Fig. 3e), and a cascade configuration (Fig. 3f).

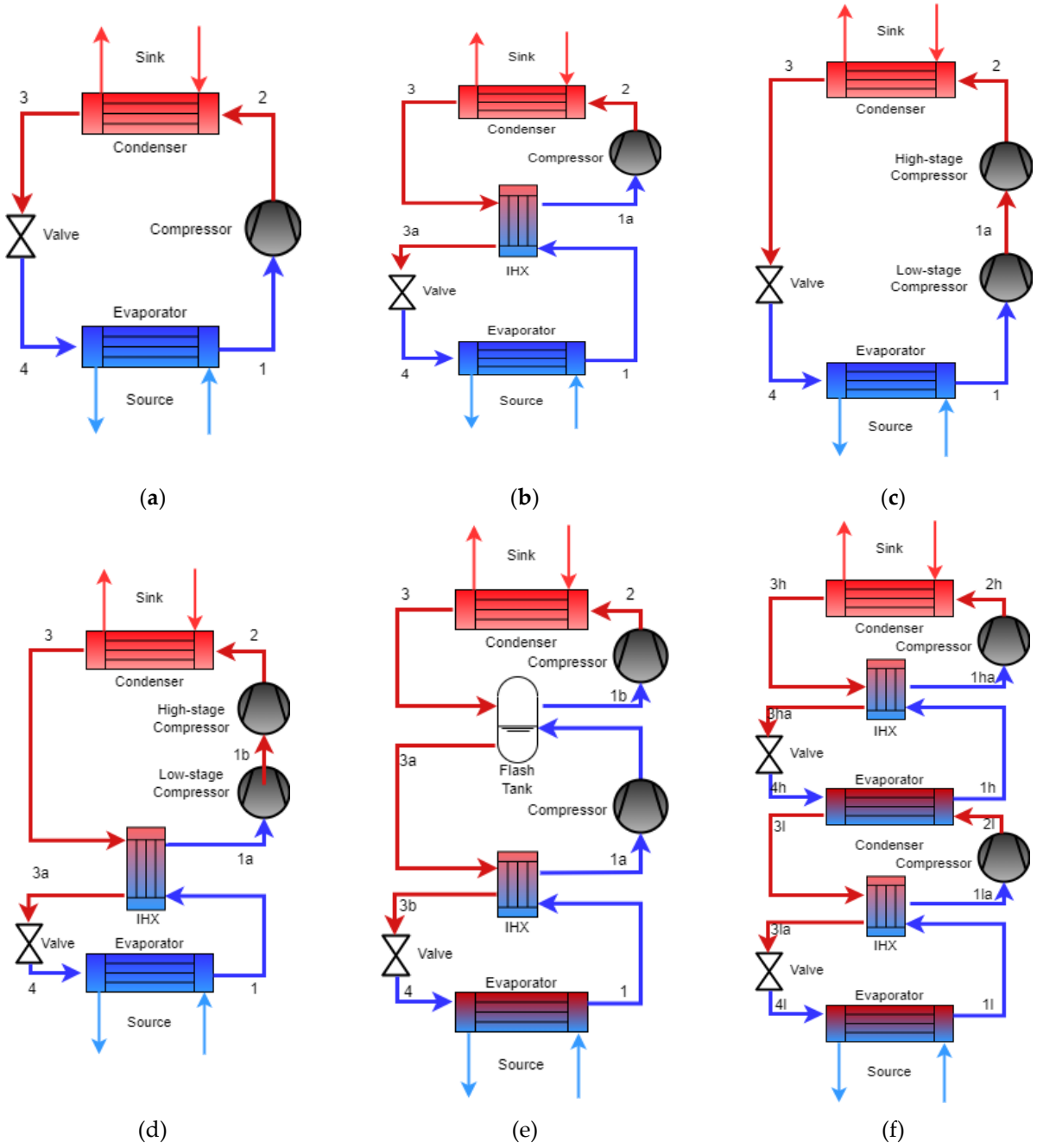

Figure. 2. *HTHP configurations analyzed: (a) SS, (b) SS-IHX, (c) TS, (d) TS-IHX, (e) TS-IHX-FT, (f) Cascade.*

Following charging, the stored thermal energy is converted back into electricity during the discharge phase. In Rankine-based Carnot batteries, the heat pump is typically coupled with an Organic Rankine Cycle (ORC), forming an integrated system. The ORC is usually implemented in a recuperative configuration, where heat from the turbine exhaust is recovered to preheat the working fluid before evaporation.

During the discharge phase, the stored heat is used to drive a recuperative Organic Rankine Cycle (ORC). The working fluid is evaporated using thermal storage as a heat source and then expanded in the turbine to generate electricity. The turbine exhaust is partially cooled in the internal heat exchanger (IHX), recovering heat to preheat the pressurized liquid stream. The fluid is subsequently condensed and pumped back to the IHX, completing the cycle.

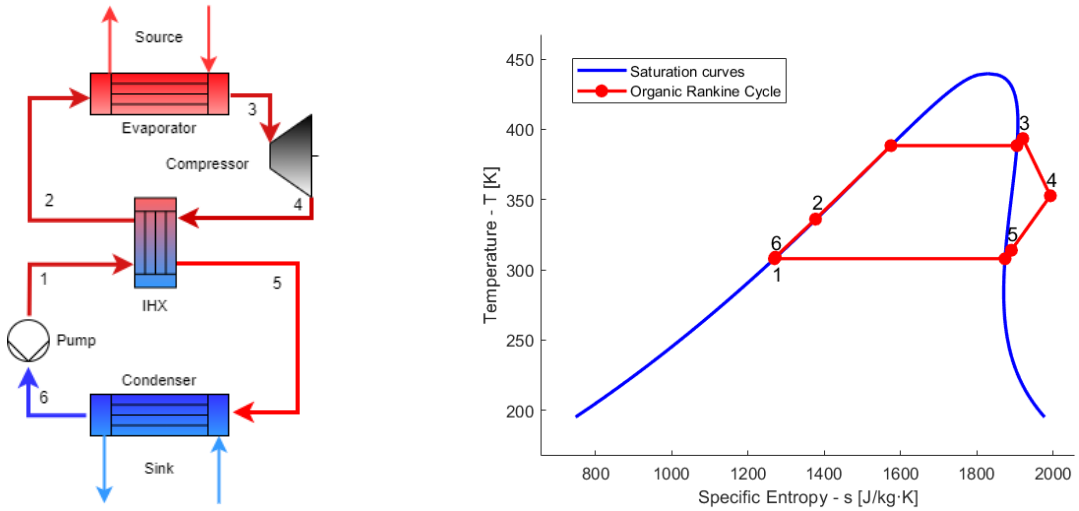

(a) (b)

Figure. 3. *Recuperative ORC configuration: (a) system layout with internal heat exchange, (b) (T–s) diagram.*

2.2. Thermodynamic modelling

A steady-state thermodynamic model of the integrated system is developed in Matlab, with thermophysical properties obtained from CoolProp [11]. The main modelling assumptions adopted in this work are:

- Steady-state operation of both HTHP and ORC;
- Negligible thermal losses from the storage tanks and heat exchangers;
- No pressure drop in pipes and heat exchangers;
- Kinetic and potential energy variations of the working fluid are neglected;
- No auxiliary electricity consumption from pumps, fans, and control sys-tems,
- Pressurized water is used as the heat-transfer fluid in the heat source, thermal storage, and cold sink.

The performance of the heat pump is evaluated using the coefficient of performance (COP) and the volumetric heat capacity (VHC), which provides an indication of system compactness. The ORC performance is assessed through its thermodynamic efficiency, while the overall Carnot battery performance is quantified by the round-trip efficiency.

$$COP = \frac{\dot{Q}_{cond,HP}}{\sum_i \dot{W}_{comp_i}} \tag{1}$$

$$VHC = \frac{\dot{Q}_{cond,HP}}{\sum_i \dot{V}_{comp,in_i}} = \frac{\dot{Q}_{cond,HP}}{\sum_i \frac{\dot{m}_{comp,in_i}}{\rho_{comp,in_i} \cdot \eta_{vol_i}}} \tag{2}$$

$$\eta_{ORC} = \frac{\dot{W}_{turb} - \dot{W}_{pump}}{\dot{Q}_{evap,ORC}} \tag{3}$$

$$\varepsilon_{rt} = COP \cdot \eta_{sto} \cdot \eta_{ORC} = \frac{\dot{W}_{el,out} \cdot \tau_{dis}}{\dot{W}_{el,in} \cdot \tau_{ch}} \tag{4}$$

The round-trip efficiency is defined considering only the electrical input to the heat pump compressor, while the waste heat is treated as an external thermal input. As a result, values exceeding unity may be obtained, reflecting the contribution of recovered waste heat to the electrical output.

Component models are based on energy balances and standard thermodynamic relations. Compressor performance accounts for isentropic and electromechanical efficiencies, while turbine efficiency is evaluated using an empirical correlation that captures off-design behaviour as a function of operating conditions. Internal heat exchangers are modelled using a minimum temperature difference approach, and expansion processes are assumed isenthalpic. The specific thermodynamic relations used to calculate the power input or output of each component are summarized in Table 1.

Table 1. *Thermodynamic equations of the HP and ORC components in the CB model.*

Component	Model	
Compressor	$\dot{W}_{comp,HP} = \sum_i \left[\frac{\dot{m}_{comp_i}\left(h_{comp,out,is_i} - h_{comp,in_i}\right)}{\eta_{OU_i} \cdot \eta_{em_i}} \right]$	(5)
	$\eta_{OU_i} = \sum_i \left[\frac{h_{comp,out,is_i} - h_{comp,in_i}}{\left(h_{ad_i} - h_{comp,in_i}\right) + v_{ad_i}\left(P_{comp,out_i} - P_{ad_i}\right)} \right]$	(6)
HP Condenser	$\dot{Q}_{cond,HP} = \dot{m}_{f,HP}\left(h_{cond,in} - h_{cond,out}\right) = \dot{m}_{sto} c_{p_{sto}} (T_{HT} - T_{LT})$	(7)
Valve	$h_{tv,in} = h_{tv,out}$	(8)
HP Evaporator	$\dot{Q}_{evap,HP} = \dot{m}_{f,HP}\left(h_{evap,out} - h_{evap,in}\right) = \dot{m}_{src} c_{p_{src}}\left(T_{src,in} - T_{src,out}\right)$	(9)
Pump	$\dot{W}_{pump} = \frac{\dot{m}_{f,ORC}\left(h_{pump,out} - h_{pump,in}\right)}{\eta_{em,pump}}$	(10)
	$\eta_{is,pump} = \frac{(h_{pump,out,is} - h_{pump,in})}{(h_{pump,out} - h_{pump,in})}$	(11)
ORC Evaporator	$\dot{Q}_{evap,ORC} = \dot{m}_{f,ORC}\left(h_{evap,out} - h_{evap,in}\right) = \dot{m}_{sto} c_{p_{sto}} (T_{HT} - T_{LT})$	(12)
Turbine	$\dot{W}_{turb} = \dot{m}_{f,ORC}\left(h_{turb,in} - h_{turb,out}\right)$	(13)
	$\eta_{is,turb} = \frac{(h_{turb,in} - h_{turb,out})}{(h_{turb,in} - h_{turb,out,is})}$	(14)
ORC Condenser	$\dot{Q}_{cond,ORC} = \dot{m}_{f,ORC}\left(h_{cond,out} - h_{cond,in}\right) = \dot{m}_{snk} c_{p_{snk}}\left(T_{snk,out} - T_{snk,in}\right)$	(15)

In the HP subsystem, the adiabatic over/under-compression efficiency is adapted from the compressor model proposed by Winandy et al. [12], Cuevas et al. [13] and, Lemort [14]. The volumetric efficiency was estimated using an empirical correlation [15] as a function of the compressor pressure ratio:

$$\eta_{vol_i} = 1.0455 - 0.0184 \cdot r_{p_i} - 0.0011 \cdot {r_{p_i}}^2 \tag{16}$$

In the ORC subsystem, the isentropic efficiency of the expander is calculated using the empirical correlation developed by Declaye et al. [16], which was originally inspired by Pacejka's equation [17] and adapted to represent the off-design behaviour of volumet-ric expanders. The correlation provides a smooth and continuous representation of the expander efficiency as a function of the pressure ratio and is expressed as:

$$\eta_{i,turb} = y_{max} \cdot sin\left\{\xi \cdot arctan\left[B \cdot \left(r_p - r_{p0}\right) - E \cdot \left(B \cdot \left(r_p - r_{p0}\right) - arctan\left(B \cdot \left(r_p - r_{p0}\right)\right)\right)\right]\right\} \tag{17}$$

The operating conditions and simulation parameters adopted in the thermodynamic model are summarized in Table 2.

Table 2. *Operating conditions and main simulation parameters of the Carnot battery system model.*

System	Parameters	Value	Units
HP	Heat source heat load ($\dot{Q}_{src}$	100	kW
	Heat source inlet temperature ($T_{src,in}$)	40-100	°C
	Heat source temperature glide ΔT_{src})	10	°C
	Superheat degree ($\Delta T_{sh,HP}$)	15	°C
	Subcooling degree ($\Delta T_{sc,HP}$)	10	°C
	Pinch point heat exchangers ($\Delta T_{pp,hx}$)	5	°C
	Storage outlet temperature (T_{HT})	90-150	°C
	Storage temperature glide (ΔT_{TES})	15	°C
	Built-in volume ratio (BVR_{comp})	3.5	-
	Compressor/turbine electromechanical efficiency (η_{em})	95	%
ORC	Cold sink outlet temperature ($T_{snk,in}$)	20	°C
	Cold sink temperature glide (ΔT_{snk})	10	°C
	Pinch point heat exchangers ($\Delta T_{pp,hx}$)	5	°C
	Superheat degree ($\Delta T_{sh,ORC}$)	5	°C
	Subcooling degree ($\Delta T_{sc,ORC}$)	0	°C
	Isentropic efficiency of the pump ($\eta_{i,pump}$)	60	°C

2.3. Working fluids

The selection of working fluids is based on thermodynamic performance and environmental considerations, with emphasis on low-GWP alternatives. The fluids considered include synthetic HFOs and HCFOs, as well as natural hydrocarbons.

Among the candidates, fluids such as R-1233zd(E) and R-1336mzz(Z) offer favourable environmental characteristics and suitable critical temperatures for high-temperature operation. Hydrocarbons such as R-600 and R-601 exhibit advantageous thermodynamic properties, particularly in terms of efficiency and volumetric performance, although their flammability requires appropriate safety considerations in practical applications.

The selected fluids provide a representative basis for evaluating trade-offs between efficiency, system compactness, and environmental impact. Table 3 summarizes the main thermophysical, environmental, and safety-related properties of the investigated working fluids

Table 3. *Thermophysical and environmental properties of low-GWP working fluids.*

Working fluid	Formula	Critical temperature, °C	Critical pressure, bar	Boiling Point, °C	ODP	GWP	Class (ASHRAE)
R245fa	C3H3F5	154.1	36.5	15.2	0	858	B1
R600	C4H10	152.0	38.0	-0.5	0	4	A3
R601	C5H12	196.6	33.7	36.1	0	20	A3
R1224yd(Z)	CF3CF=CHCl	155.5	33.4	14.6	0	<1	A1
R1233zd(E)	CF3CH=CHCl(E)	166.5	36.2	18.3	0	1	A1
R1234ze(Z)	CHF=CHCF3(Z)	150.1	35.3	9.7	0	1	A2L
R1336mzz(Z)	CF3CH=CHCF3 (Z)	171.4	29.0	33.5	0	2	A1

3. Results

Section 3.1 presents a parametric analysis of the heat pump key performance indicators (KPIs), namely the coefficient of performance and the volumetric heat capacity, as a function of the temperature lift under two operating scenarios: (i) a fixed high-temperature storage level and (ii) a fixed waste-heat source temperature. In addition, the influence of the ORC efficiency (η_{ORC}) and the overall round-trip efficiency (ε_{rt}) is investigated. Subsequently, in Section 3.2, a single-objective optimization is performed to evaluate the performance of the different system configurations and working-fluid combinations, using the round-trip efficiency as the objective function, for three representative waste-heat source temperatures typical of different industrial sectors.

3.1. Parametric Analysis

As shown in Figure 4(a), the COP decreases with increasing temperature lift for all configurations, primarily due to the increase in compression work associated with higher pressure ratios. At low temperature lifts, single-stage configurations, particularly SS-IHX, exhibit the highest performance. The internal heat exchanger is particularly advantageous, as the added subcooling in-creases the condensation enthalpy difference without significantly penalizing the compression work. However, as the temperature lift increases, two-stage and cascade configurations become more favourable, as they reduce compression losses through pressure ratio splitting and intercooling effects. At a temperature lift of 80 K, these configurations converge to COP values of approximately 3.0 to 3.1, while the SS-IHX and SS decrease to around 2.4 and 2.0, respectively.

Figure 4(b) highlights the impact of working fluid selection. At low temperature lifts, fluids such as R-601 achieve higher COP values, while at higher lifts the performance differences among fluids tend to diminish, with R-600 showing a slight advantage under more demanding conditions.

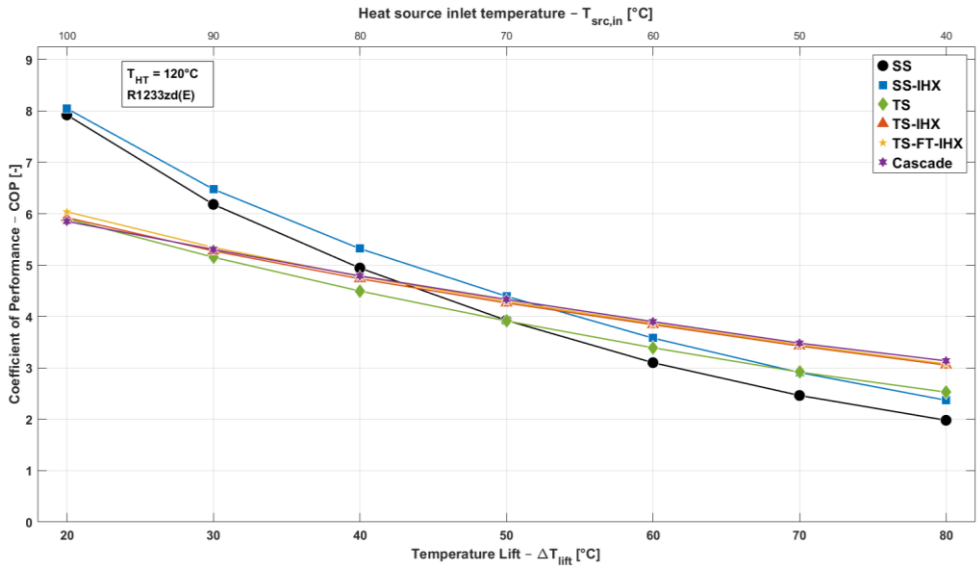

(a)

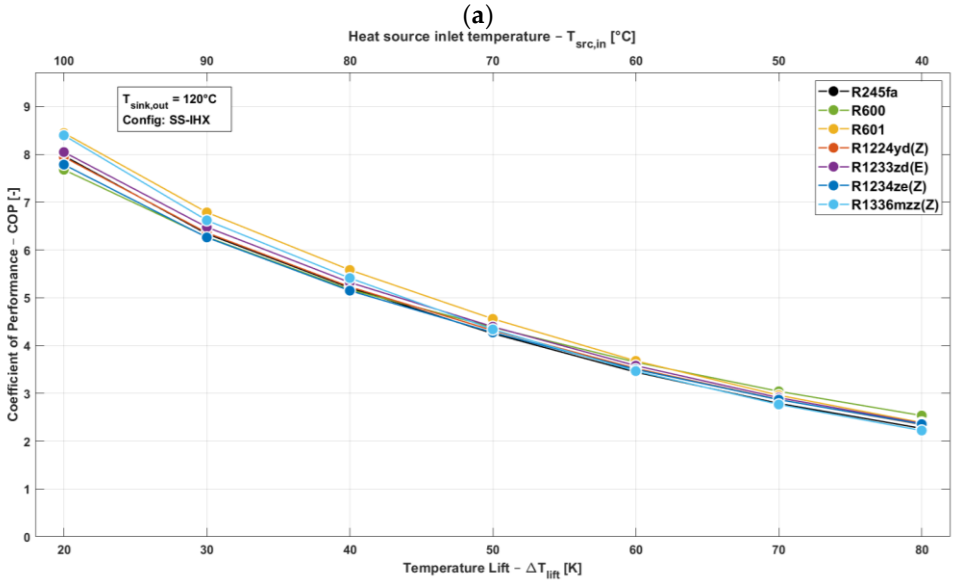

(b)

Figure. 4. *Coefficient of performance (COP) as a function of temperature lift: (a) comparison of heat pump configurations; (b) comparison of working fluids (SS-IHX).*

The corresponding trends for volumetric heat capacity are presented in Figure 5. As shown in Figure 5(a), VHC decreases with increasing temperature lift for all configurations, reflecting the combined effect of reduced suction density and lower volumetric efficiency at higher pressure ratios. In contrast to COP, single-stage configurations maintain superior volumetric performance over a wider operating range. The superiority of the SS-IHX over the basic SS cycle arises from the additional sub-cooling provided by the internal heat exchanger, which increases the condensation enthalpy difference and, consequently, the volumetric heating capacity.

Figure 5(b) shows that the ranking of working fluids is largely reversed compared to COP. R-600 consistently exhibits the highest VHC due to its higher vapor density at compressor suction, while R-601 presents significantly lower values, indicating larger compressor size requirements. Notably, this ranking remains essentially unchanged as the temperature lift increases, indicating that the influence of refrigerant volatility on volumetric performance is preserved across the entire operating range.

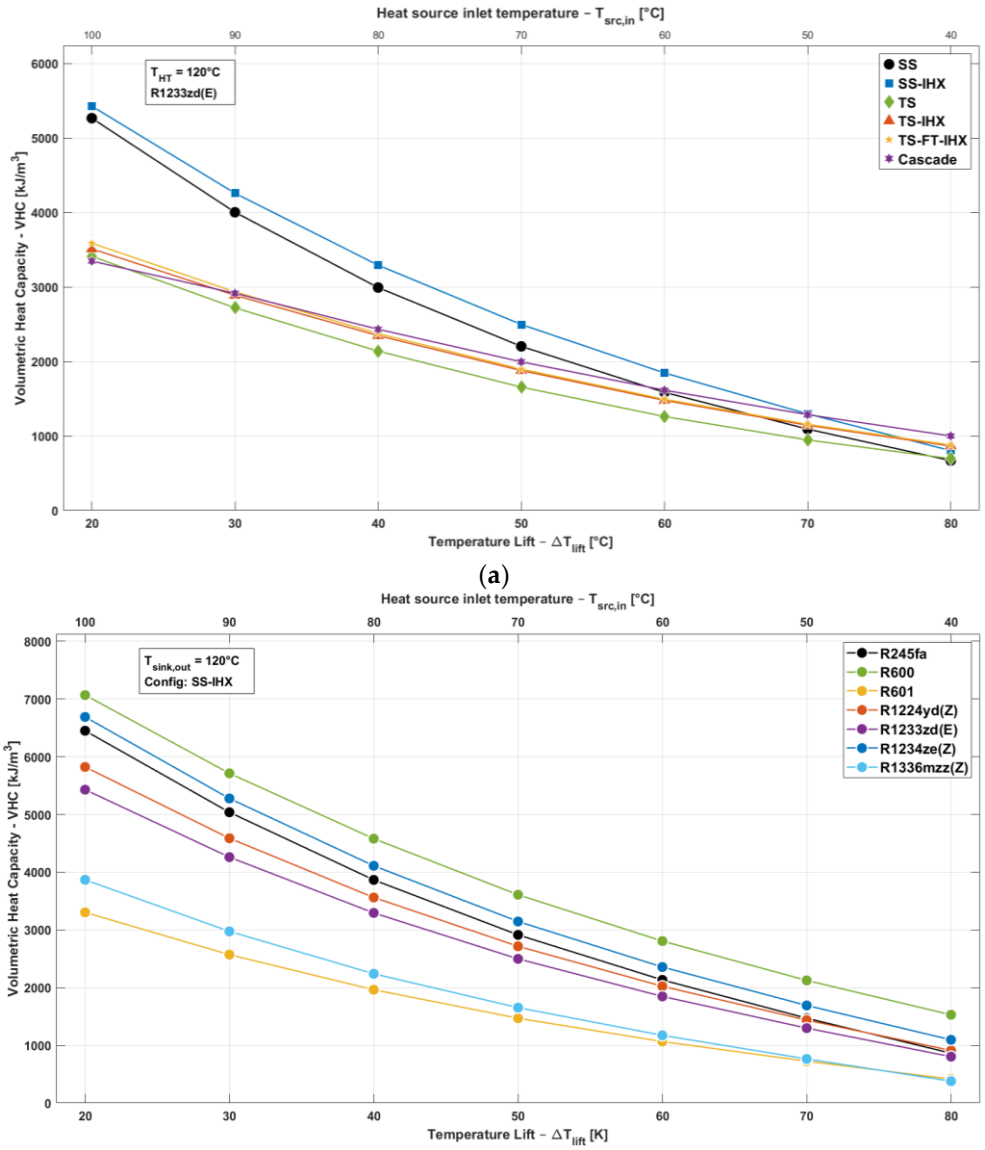

Figure. 5. *Volumetric heat capacity (VHC) as a function of temperature lift: (a) comparison of heat pump configurations; (b) comparison of working fluids (SS-IHX).*

To analyse the behaviour of the discharging subsystem, the performance of the recuperative Organic Rankine Cycle is evaluated as a function of the storage outlet temperature for different working fluids. Figure 6a illustrates the variation of the ORC thermodynamic efficiency with increasing storage temperature, while Figure 6b provides additional insight into the underlying turbine behaviour by showing the evolution of turbine work output, pressure ratio, and isentropic efficiency.

The ORC efficiency generally increases with storage outlet temperature due to the larger temperature difference available for heat addition, which enhances turbine work. Among the fluids, R-601 achieves the highest efficiency at elevated temperatures, while R-600 performs better at lower temperatures but converges toward similar performance at higher levels, as showed in Figure 8(a).

However, the efficiency improvement becomes less pronounced at higher temperatures. As illustrated in Figure 8(b), although the turbine pressure ratio and work output continue to increase, the isentropic efficiency reaches a maximum and then declines due to off-design operation and over-expansion effects. This reduction in turbine efficiency partially offsets the gains in work output, leading to diminishing improvements in overall ORC performance.

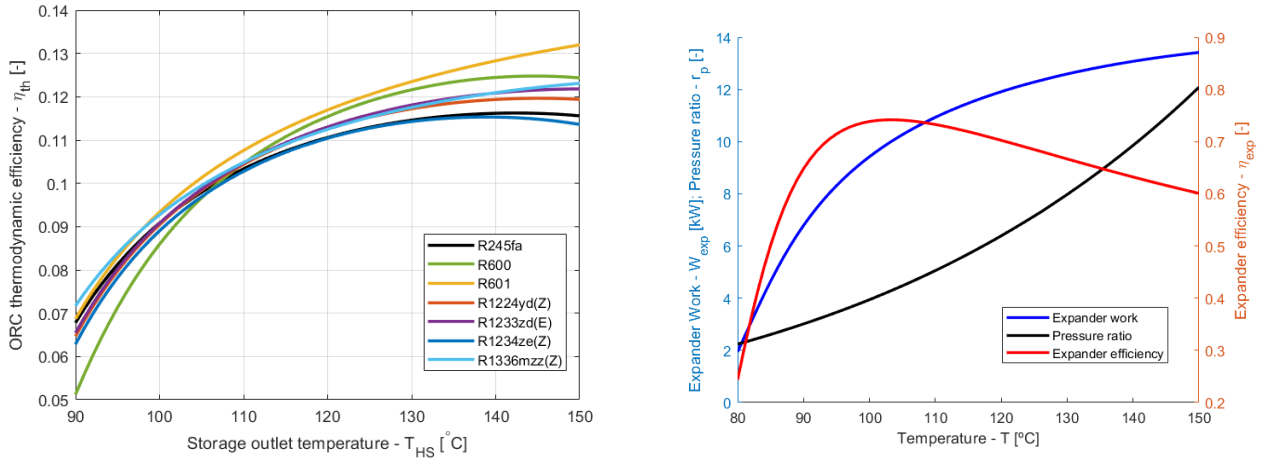

(**a**) (**b**)

Figure. 6. *Volumetric heat capacity (VHC) as a function of temperature lift: (a) comparison of heat pump configurations; (b) comparison of working fluids (SS-IHX).*

3.2. Roundtrip efficiency optimization

The overall performance of the Carnot battery is assessed through the round-trip efficiency, which captures the combined effect of charging and discharging processes. In this section, the round-trip efficiency is evaluated as a function of storage outlet temperature and waste heat source temperature to identify optimal system configurations across a wide operating range. A grid-search optimization is performed by varying the storage outlet temperature (90–150 °C) and the waste heat source temperature (40–100 °C). The operating domain is discretized, and only thermodynamically feasible points are considered, ensuring realistic cycle operation and avoiding extreme conditions such as near-critical states or excessive compression ratios. For every combination of storage outlet temperature and waste heat source temperature, all candidate heat-pump configurations are systematically evaluated, and the round-trip efficiency is maximized by selecting the best-performing architecture. This approach enables the identification of both the optimal heat-pump configuration and the corresponding maximum achievable round-trip efficiency under the pre-scribed thermal boundary conditions.

The first column of Figure 7 illustrates the optimal heat pump configuration selected through grid-search optimization as a function of the storage outlet temperature and waste heat source temperature. The second column of Figure 7 presents the corresponding maximum round-trip efficiency achieved at each operating point.

The results show that the optimal heat pump configuration depends on the combined effect of storage outlet temperature and waste heat source temperature. At low temperature lifts, corresponding to high source temperatures and low storage temperatures, single-stage configurations are preferred. As the temperature lift increases, the optimal solution shifts towards two-stage and cascade configurations, which reduce compression losses through pressure ratio splitting and intercooling effects. The round-trip efficiency generally increases with higher waste heat source temperatures and decreases with increasing storage outlet temperature. Higher source temperatures improve heat pump performance by reducing compression work, while higher storage temperatures impose larger temperature lifts and increase irreversibilities in both subsystems.

Comparing the working fluids, R-601 achieves higher round-trip efficiencies at elevated storage temperatures, reflecting its suitability for high-temperature applications. In contrast, R-1233zd(E) exhibits a more balanced performance across the operating range, with smoother variations and robust behaviour under different conditions.

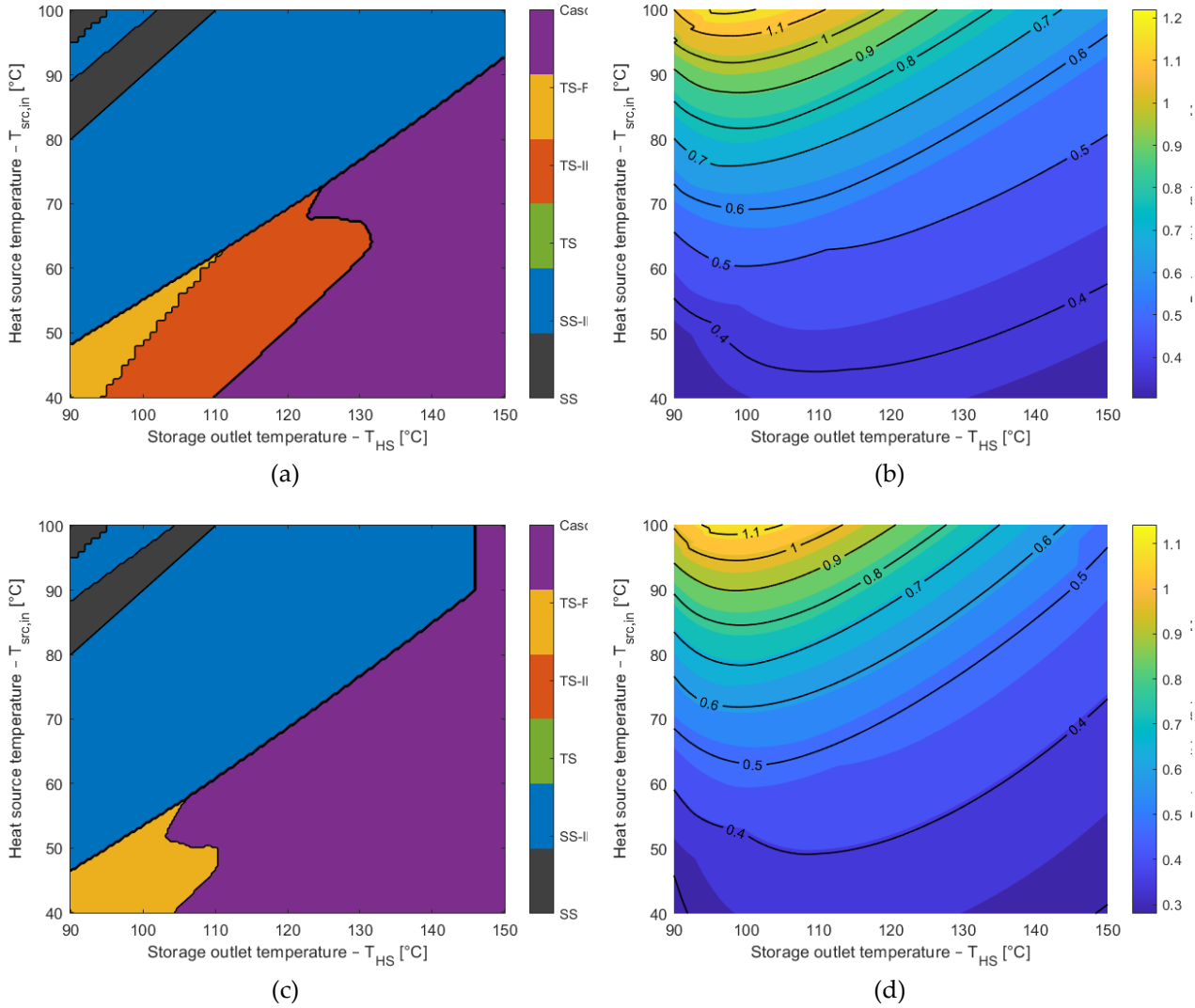

Figure. 7. *Carnot battery performance as a function of storage outlet and waste heat source temperatures: (a) optimal HP configuration for R-601; (b) maximum RTE for R-601; (c) optimal HP configuration for R-1233zd(E); (d) maximum RTE for R-1233zd(E).*

Following the operating maps presented in Figure 11, the optimal operating conditions for the selected working fluids are summarized in Table 4. The table reports the combination of waste heat source inlet temperature and storage outlet temperature that maximizes the round-trip efficiency, together with the corresponding heat pump configuration and key performance indicators. This representation complements the contour maps by providing a concise overview of the best-performing operating points.

Table 4. Optimal operating conditions and performance indicators of the Carnot battery.

Fluid	$T_{src,in}$ [°C]	T_{HT} [°C]	VHC	COP [-]	η_{ORC} [%]	ε_{rt} [-]	HP Config
R245fa	100	95	7.67	14.81	8.12	1.2035	SS-IHX
R600	100	102	7.94	11.52	9.06	1.0435	SS-IHX
R601	100	97	3.70	13.96	8.75	1.2205	SS-IHX
R1224yd(Z)	100	96	6.83	14.13	8.22	1.1608	SS-IHX
R1233zd(E)	100	97	6.24	13.46	8.48	1.1424	SS-IHX
R1234ze(Z)	100	97	7.85	13.42	8.30	1.1138	SS-IHX
R1336mzz(Z)	100	95	4.48	15.49	8.39	1.2989	SS-IHX

4. Conclusions

This work presented a thermodynamic assessment of a Rankine-based Carnot battery integrating different high-temperature heat pump (HTHP) configurations with a recuperative Organic Rankine Cycle (ORC),

considering waste heat recovery and low-GWP working fluids. The main findings can be summarized as follows:

- Heat pump configuration has a dominant impact on system performance. Specifically, single-stage configurations with internal heat exchange provide the best performance at low to moderate temperature lifts, while two-stage and cascade configurations become advantageous at higher temperature lifts by reducing compression losses.
- Working fluid selection introduces a trade-off between efficiency and compactness. While R-601 achieves higher round-trip efficiencies, particularly at elevated storage temperatures, R-1233zd(E) provides a more balanced performance with improved volumetric characteristics and operational flexibility.
- The ORC performance benefits from increasing storage temperature but is limited by turbine off-design behavior. Although higher temperatures increase turbine work, efficiency gains are reduced at high operating conditions due to over-expansion effects.
- Grid-search optimization of the complete Carnot battery revealed that no single configuration or working fluid is universally optimal. The selection of heat pump configuration and working fluid varies with the combination of storage temperature and waste heat source temperature, highlighting the need for integrated system-level optimization.
- The obtained results confirm the potential of HP–ORC Carnot batteries for industrial applications, particularly when high-temperature waste heat is available.

Under the operating conditions investigated, the electric round-trip efficiency of the Carnot battery ranges approximately between 1.04 and 1.30, depending on the working fluid and operating temperatures. It should be noted that this metric represents an electric-to-electric efficiency with waste-heat assistance, where only the electrical input to the heat pump compressor is considered in the denominator while the waste heat supplied to the evaporator acts as an external thermal co-input. Consequently, values exceeding unity do not violate thermodynamic principles but reflect the additional electrical power generated from the upgraded waste heat.

Overall, the results demonstrate that high-performance Carnot battery design requires a combined optimization of system architecture, working fluid, and operating conditions. The presented analysis provides practical guidance for the integration of waste-heat-assisted Carnot batteries in industrial energy systems.

Acknowledgments

This work was funded by the Fundo Europeu de Desenvolvimento Regional (FEDER) through the Thematic Programme Innovation and Digital Transition (COMPETE 2030), under Portugal 2030, and by the European Union, via the Fundação para a Ciência e a Tecnologia (FCT), within the framework of Project No. 17137 | COMPETE2030-FEDER-00854000.

Nomenclature

Abbreviations

BVR	Built-in volume ratio
CB	Carnot battery
COP	Coefficient of performance
GWP	Global worming potential
HP	Heat pump
HT	High temperature
HTHP	High temperature heat pump
IHX	Internal heat exchanger
KPI	Key performance indicators
LT	Low temperature
ORC	Organic Rankine cycle
RTE	Roundtrip efficiency
PTES	Pumped thermal energy storage
SS	Single stage
TES	Thermal Energy Storage
TS	Two-stage
VHC	Volumetric heat capacity

Subscripts:

Symbols:

E	Electrical energy
h	Specific enthalpy (kJ/kg)
$\dot{m}$	Mass flow rate (kg/s)
N	Rotational speed (rpm)
r_p	Pressure ratio (-)
p	Pressure (kPa, abs.)
P	Power (W)
$\dot{Q}$	Heat transfer rate (W)
s	Specific entropy (kJ/kg.K)
T	Temperature (°C)
$\dot{W}$	Mechanical power (W)
x	Vapor quality (-)

Greek letters:

ρ	Density (kg/m^3)
Δ	Variation (-)
η	Efficiency (-)
τ	Time duration (s)
ε	Efficiency (-)

ad	charge
ch	charge
cond	Condenser
cold	Cold
comp	Compressor
dis	discharge
el	Electric
em	Electro-magnetic
evap	Evaporator
exp	turbine
f	Working fluid
ft	Flash tank
hot	Hot
in	Inlet
is	Isentropic
liq	Liquid
ou	Over-under
out	Outlet
pp	Pinch point
pump	Pump
rt	Roundtrip
sat	saturation
sc	Subcooling
sh	Superheating
snk	Sink fluid
src	Source fluid
sto	Storage fluid
turb	turbine
tv	Throttle valve
vap	Vapor
vol	Volumetric

References

[1] Dumont, O.; Frate, G.F.; Pillai, A.; Lecompte, S.; De paepe, M.; Lemort, V. Carnot Battery Technology: A State-of-the-Art Review. J. Energy Storage 2020, 32, doi:10.1016/j.est.2020.101756.

[2] Liang, T.; Vecchi, A.; Knobloch, K.; Sciacovelli, A.; Engelbrecht, K.; Li, Y.; Ding, Y. Key Components for Carnot Battery: Technology Review, Technical Barriers and Selection Criteria. Renewable and Sustainable Energy Reviews 2022, 163

[3] Santos, M.; André, J.; Mendes, R.; Ribeiro, J.B. Multi-Objective Optimization of a Carnot Battery System for Energy Storage. In Proceedings of the Proceedings of ECOS 2024; pp. 778–787.

[4] Santos, M.; André, J.; Mendes, R.; Ribeiro, J.B. Thermo-Economic Optimization of a Carnot Battery under Transient Conditions. In Proceedings of the ECOS 2023, 2023; pp. 2171–2182.

[5] Frate, G.F.; Antonelli, M.; Desideri, U. A Novel Pumped Thermal Electricity Storage (PTES) System with Thermal Integration. Appl. Therm. Eng. 2017, 121, 1051–1058

[6] .Dumont, O.; Lemort, V. Mapping of Performance of Pumped Thermal Energy Storage (Carnot Battery) Using Waste Heat Recovery. Energy 2020, 211

[7] Zhou, T.; Shi, L.; Sun, X.; Zhang, M.; Zhang, Y.; Yao, Y.; Pan, Z.; Hu, Q.; Jiang, Z.; Tian, H.; et al. Performance Enhancement of Thermal-Integrated Carnot Battery through Zeotropic Mixtures. Energy 2024, 311

[8] Frate, G.F.; Ferrari, L.; Desideri, U. Multi-Criteria Investigation of a Pumped Thermal Electricity Storage (PTES) System with Thermal Integration and Sensible Heat Storage. Energy Convers. Manag. 2020, 208

[9] Zhang, Y.; Xu, L.; Li, J.; Zhang, L.; Yuan, Z. Technical and Economic Evaluation, Comparison and Optimization of a Carnot Battery with Two Different Layouts. J. Energy Storage 2022, 55

[10] Eppinger, B.; Zigan, L.; Karl, J.; Will, S. Pumped Thermal Energy Storage with Heat Pump-ORC-Systems: Comparison of Latent and Sensible Thermal Storages for Various Fluids. Appl. Energy 2020, 280

[11] Bell, I.H.; Wronski, J.; Quoilin, S.; Lemort, V. Pure and Pseudo-Pure Fluid Thermophysical Property Evaluation and the Open-Source Thermophysical Property Library CoolProp. Ind. Eng. Chem. Res. 2014, 53, 2498–2508

[12] Winandy, E.; O, C.S.; Lebrun, J. Experimental Analysis and Simplified Modelling of a Hermetic Scroll Refrigeration Compressor. 2002, 22, 107–120

[13] Cuevas, C.; Lebrun, J.; Lemort, V.; Winandy, E. Characterization of a Scroll Compressor under Extended Operating Conditions. Appl. Therm. Eng. 2010, 30, 605–615

[14] Lemort, V.; Quoilin, S.; Cuevas, C.; Lebrun, J. Testing and Modeling a Scroll Expander Integrated into an Organic Rankine Cycle. Appl. Therm. Eng. 2009, 29, 3094–3102

[15] Mateu-Royo, C.; Arpagaus, C.; Mota-Babiloni, A.; Navarro-Esbrí, J.; Bertsch, S.S. Advanced High Temperature Heat Pump Configurations Using Low GWP Refrigerants for Industrial Waste Heat Recovery: A Comprehensive Study. Energy Convers. Manag. 2021, 229

[16] Declaye, S.; Quoilin, S.; Guillaume, L.; Lemort, V. Experimental Study on an Open-Drive Scroll Expander Integrated into an ORC (Organic Rankine Cycle) System with R245fa as Working Fluid. Energy 2013, 55, 173–183

[17] Pacejka, H.B.. Tyre and Vehicle Dynamics; Butterworth-Heinemann, 2006; ISBN 9780750669184